ORAL/POSTER REFERENCE: ICF100495OR

DAMAGE INITIATION AND EVOLUTION IN A HETEROGENEOUS MATERIAL

C. Liu[1], M.G. Stout[1] and B.W. Asay[2]

[1]MST-8, Materials Science and Technology Division
[2]DX-2, Dynamic Experimentation Division
Los Alamos National Laboratory
Los Alamos, NM 87545, USA

ABSTRACT

Heterogeneity and heterogeneity-induced damage in a high explosive simulant material are studied. In contrary to common practice, where it is assumed that the uniaxial compression sample is undergoing homogeneous deformation, we find that the strain field within the sample at each loading level is a distribution due to the heterogeneous nature of the material. As deformation proceeds, this distribution evolves, which indicates the initiation and evolution of damage. It is also shown that damage initiation occurs well before the applied load reaches its maximum value. The driving force that triggers the initiation of damage is identified and estimated based on a theory that explicitly treats the high explosive as a heterogeneous composite.

KEYWORDS

Heterogeneity, heterogeneity-induced damage, damage initiation, and damage evolution.

INTRODUCTION

High explosive (HE) materials are heterogeneous at the microscopic level and this heterogeneity plays a vital role in attaining the desired structural response in such areas as strength, stiffness, constitutive response, and fracture resistance. Consequently, the ability of providing accurate quantitative estimates of the constitutive behavior and flaw tolerance of HE materials is a direct concern for safety. HE materials, such as the PBX 9501, are composed by two phases: the energetic crystal and the polymeric binder. Under uniaxial loading, we found that the responses of the PBX 9501 high explosive in tension and in compression are quite different. In tension, the PBX 9501 specimen fails at relatively low strain level and failure occurs in a very narrow band normal to the loading axis. This behavior is similar to that of typical brittle solids. In compression, failure happens at relatively high strain level. Failure is also accompanied by massive internal cracking and the majority of the crack is parallel to the loading axis. The Poisson's ratio, as usually defined, is found to be an increasing function of the total axial deformation before the load reaches maximum value. Based on the conventional uniaxial stress test, if the PBX 9501 is viewed as homogeneous, there will be no driving force to generate the cracks observed in experiments. This concludes that the conventional way of conducting and interpreting uniaxial stress experiment cannot provide any explanation of what we see in the experiment. It is the objective of this investigation to observe the initiation and evolution of damage in a

high explosive simulant material under uniaxial compression, and to identify the driving forces that trigger the damaging process.

MATERIAL DESCRIPTION AND TESTING TECHNIQUE

A high explosive simulant material, referred to as PBS 9501, was used in the present investigation. The PBS 9501 simulant material is composed of 94wt% C&H granulated sugar and 6wt% polymeric binder, which in turn, is composed by 50% estane and 50% nitroplasticizer. The reason of choosing such a material is that PBS 9501 can simulate, at the macroscopic level, the mechanical behavior of the PBX 9501 high explosive, which is composed by the HMX energetic crystal and a polymeric binder, as a function of strain rate and temperature. Also, the sugar crystal and the HMX crystal are both monoclinic, so they are similar microscopically as well. Both the PBS 9501 and the PBX 9501 have the same polymeric binder system.

When a heterogeneous material is subjected to homogeneous boundary condition, below certain length scale, the deformation field will become non-uniform due to the heterogeneous nature of the material. Hence, to experimentally study the heterogeneity and heterogeneity-induced damage, one would need a technique that is able to monitor the full-field deformation throughout the entire sample. We developed an optical technique called dot-matrix deposition & mapping. In principle, this technique is very similar to the image correlation method [1], but avoids the ambiguity regarding the reflectivity of the specimen surface during the deformation process, especially, when damage is involved. Before experiment, a matrix of dot pattern is deposited on the surface of the specimen and the pattern is photographed at different moments during deformation. One of such photographs is shown in Figure 1(a). This image is then processed to

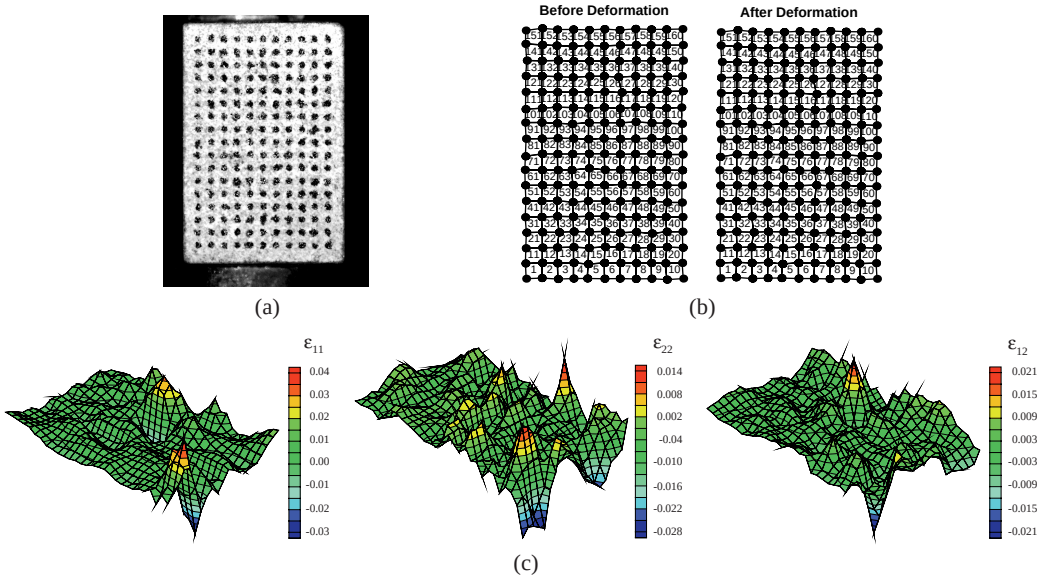

Figure 1: Dot-matrix deposition & mapping technique.

identify the exact location of the center of each dot. Based on the coordinates of each dot, an element mesh, as shown in Figure 1(b), for the moments of before and after deformation can be constructed. By assuming that each element is undergoing homogeneous deformation, all three in-plane strain components can be calculated using the coordinates of those four nodes. The field plot for each strain component that corresponds to the deforming state in Figure 1(b) is shown in Figure 1(c). The formulation for obtaining the strain components of each element is valid for finite deformation. Therefore, the technique we developed in this study is able to deal with local large deformation associated with damage.

EXPERIMENTAL OBSERVATIONS

The specimen we studied has a rectangular shape with the width and the thickness of 12.7mm. The height of the sample is 19.0mm. The specimen was loaded in compression at an equivalent strain rate of

$1.7\times10^{-4}\,\mathrm{sec}^{-1}$. The size of the element as shown in Figure 1(b) is about $1\mathrm{mm}\times1\mathrm{mm}$. Based on the technique described in the previous section, in-plane strain components of each element are calculated at each loading level. In the following we only present the result for the lateral strain component ε_{11}.

In Figure 2, the lateral strain component ε_{11}, at two moments during the early stage of loading is shown. One plot is a scatter plot showing the strain magnitude of each element and the other is a distribution plot showing the percentage of elements that experience certain strain. If the material is indeed homogeneous,

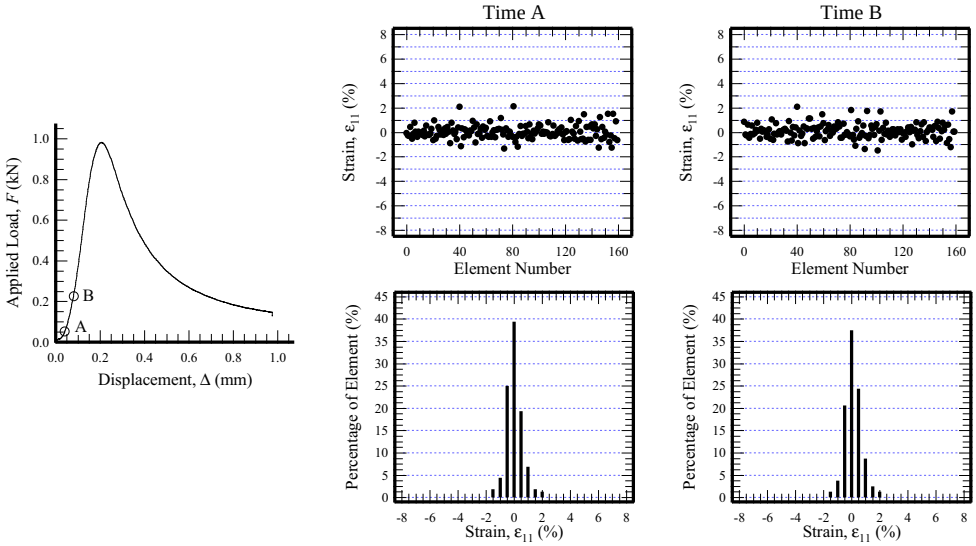

Figure 2: Strain distribution showing heterogeneous deformation during early stage of loading.

every element should deform exactly the same amount at the same time. Therefore, for a homogeneous material, all the data points in the scatter plot should fall on a horizontal line, and in the distribution plot we will only have a vertical line. However, in Figure 2, we can see that the deformation of the elements is scattered around a mean value. Also for the early stage of loading the overall shape of the distribution plot remains the same; only the mean value shifts responding to the overall deformation the entire specimen being subjected to. The shape of strain distribution, therefore, indicates the heterogeneous nature of the material. Note that the size of the element is about $1\mathrm{mm}\times1\mathrm{mm}$, which is much larger than the average diameter of the crystals.

In Figure 3, we study two consecutive moments along the loading curve. At time C, the compressive load is

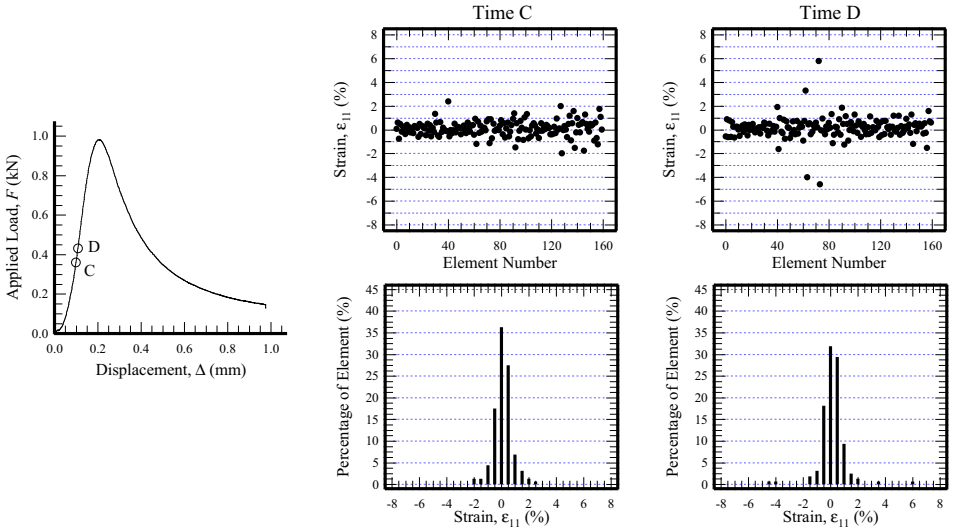

Figure 3: Indication of damage initiation in the specimen under compression.

360N and at time D, the compressive load increases to 432N. During such a small increment of loading, the distribution of the lateral strain component ε_{11} exhibits a drastic change that indicates the initiation of

damage within the test specimen. At time C, the shape of the distribution of ε_{11} is the same as those shown in Figure 2. At time D, several elements experience a much larger strain compared to the rest of elements. Two of these elements experience larger tensile strain and other two experience larger compressive strain. Simple analysis showed that the cracking of a material element under compression causes additional strain increment in the lateral direction. Therefore, those two elements that exhibit larger tensile strain must also experience cracking within the elements. At time D, where damage initiation is detected, the compressive stress $\sigma = 0.44\sigma_C$ where σ_C is the compressive strength of the material. Also, note that the two elements that experience a larger compressive strain are located next to the ones that exhibit larger tensile strain. When internal cracking occurs in an element, it will tend to expand more in the lateral direction. As a result, the element next to the cracked element has to be compressed in order to keep the overall deformation compatible.

Another observation can be made based on the results shown in Figure 3. At time D, if we ignore the elements that exhibit larger strains compared to other elements, we find that the distribution of the strain component ε_{11} is similar to that at previous moments. This suggests that the damage is confined within the individual element. On the other hand, if the region of damage extends over several elements, we will see a change in the overall shape of the strain distributions. This is demonstrated in Figure 4 where strain

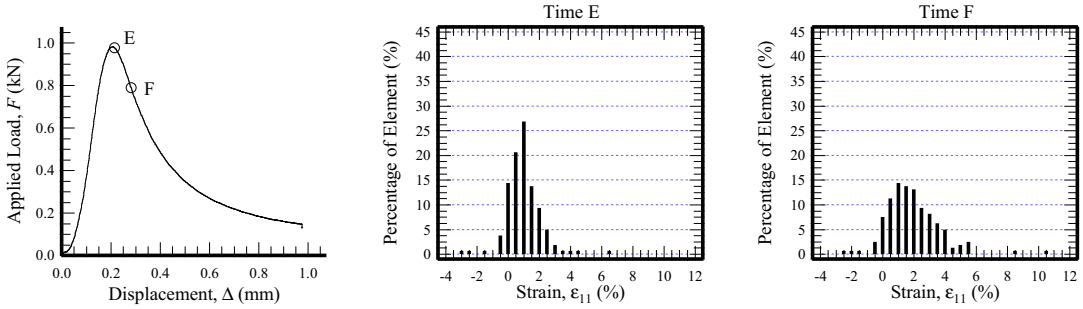

Figure 4: Indication of damage accumulation and evolution in the specimen under compression.

distributions at times after damage initiation. As a result, the broadness of the strain distribution provides a mean for monitoring damage evolution in the specimen.

DISCUSSIONS

Many theoretical investigations were conducted to explain the appearance of the splitting cracks in compression of brittle solids, e.g., [2]. These theories require pre-existing cracks within the sample. Although in most of brittle materials, microcracks do exist prior to the loading due to processing, the accurate description of the distribution of cracks proves to be very difficult if not impossible. Meanwhile, most of these micromechanical analyses treat the matrix material as homogeneous. From the experimental observations shown in previous section, we see that the strain distribution clearly indicates the heterogeneous nature of the material prior to the initiation of damage. It would be more appropriate of applying a theory, which treats the simulant material as a heterogeneous composite, to study the initiation of damage in compression.

Ortiz [3] proposed a general framework for the constitutive modeling of concrete starting from the first principles of mechanics based on the theory of interacting continua or mixture theory, and a rate-independent theory of damage. An important feature of this framework is that the concrete is treated explicitly as a mixture comprising two distinct phases: mortar and aggregate. A conclusion of this framework is that the externally applied stresses distribute unequally between the two phases. The average stresses acting in mortar and aggregate must jointly equilibrate the applied loads but may be vastly different from each other. Here we will adopt a very simple version of this mixture theory to show that purely compressive uniaxial load will induce tensile stress normal to the loading axis within the crystal, and the tensile stress is high enough to initiate damage before the overall compressive load reaches its peak value.

Consider a material element where the volumetric fractions of the crystal and the binder are f_1 and f_2, respectively. Let σ_1 and σ_2 be the average or phase stresses acting in crystal and binder, and σ the applied stress. The requirement that σ_1 and σ_2 jointly equilibrate σ can be expressed as

$$\sigma = f_1\sigma_1 + f_2\sigma_2 . \tag{1}$$

In order to make it more apparent about the fact that lateral tensile stress can be induced when HE material is subjected to uniaxial compression we consider a "virgin" HE specimen and assume that both crystal and binder are isotropic and elastic. As a result, the phase stresses σ_1 and σ_2 can be related to the applied stress σ through

$$(\sigma_\alpha)_{ij} = \frac{1}{3}\left(\frac{k_\alpha}{k} - \frac{\mu_\alpha}{\mu}\right)\sigma_{mm}\delta_{ij} + \frac{\mu_\alpha}{\mu}\sigma_{ij}, \qquad \alpha = 1,2, \tag{2}$$

where k_α and μ_α are the bulk and shear moduli of each constituent and k and μ are the bulk and shear moduli for the composite. Under uniaxial compression, where external stress is characterized by $\sigma_{ij} = -\sigma\delta_{i1}\delta_{j1}$ and $\sigma > 0$ is the magnitude of the applied compressive stress, the phase stress within crystal σ_1 has the following form

$$(\sigma_1)_{ij} = \begin{bmatrix} \sigma_{\mathrm{L}} & 0 & 0 \\ 0 & \sigma_{\mathrm{T}} & 0 \\ 0 & 0 & \sigma_{\mathrm{T}} \end{bmatrix}, \qquad \sigma_{\mathrm{L}} = -\frac{1}{3}\left(\frac{k_1}{k} + \frac{2\mu_1}{\mu}\right)\sigma, \qquad \sigma_{\mathrm{T}} = \frac{1}{3}\left(\frac{\mu_1}{\mu} - \frac{k_1}{k}\right)\sigma. \tag{3}$$

Experimental measurements have shown that the binder material is almost incompressible, i.e., its Poisson's ratio $\nu_2 \approx 0.5$. Then, one can show that

$$\frac{\sigma_{\mathrm{T}}}{\sigma} = \frac{1}{3f_1}\left\{1 + \frac{2(1+\nu_1)}{3}\cdot\frac{f_2E_2}{f_1E_1}\right\}^{-1}, \tag{4}$$

where ν_1 is the Poisson's ratio of the crystal, E_1 and E_2 are the Young's modulus of crystal and binder, respectively. For the simulant material PBS 9501, $f_1 \approx 0.96$ and the Poisson's ratio of crystal $\nu_1 \approx 0.2$. Meanwhile, within a wide strain-rate regime, the ratio of E_2/E_1 is in the order of 10^{-3}. As a result, the second term in the braces of the above expression is negligible that leads to $\sigma_{\mathrm{T}}/\sigma \approx 1/3f_1 = 0.35$. One can also show that the lateral stress within the binder is almost zero.

In a typical uniaxial compression test of the PBS 9501, the apparent stress-strain curve is shown as the solid line in Figure 5. The applied uniaxial stress is a monotonic increasing function of the axial strain before reaching the maximum value. After this point, stress decreases gradually as the deformation continues to proceed. If we take a crystal element from the compressive sample, the phase stress within the crystal is characterized by σ_{L}, compressive and parallel to the externally applied load and by σ_{T}, tensile and normal to the loading axis. The variation of the lateral tensile stress σ_{T} is shown as dash-dotted line in the figure. Experimental measurement also showed that the tensile strength of the PBS 9501 material is only about 15% of its compressive strength. If we assume that in tension, failure is mainly due to crystal cracking, we may conclude that microcracks start to develop in crystals when $\sigma_{\mathrm{T}} \approx 0.15\sigma_{\mathrm{C}}$. The onset strain for microcrack initiation within the compressive sample is indicated by the vertical dash-line in the figure. Therefore, damage initiation would occur when the compressive stress $\sigma \approx 0.42\sigma_{\mathrm{C}}$. This prediction matches the experimental observation shown in Figure 3 very well.

Immediately after damage initiation, microcracks within the sample are so few that they do not interact with each other. The enlargement of those cracks remains stable due to stress redistribution between crystal and binder, and the applied stress keeps increasing as deformation proceeds. However, when the size or the

density of microcracks becomes large enough that the stress redistribution cannot ensure stable crack growth any more, unstable crack propagation follows and this is the direct cause of the characteristic descending branch of the uniaxial compressive stress-strain curve in Figure 5.

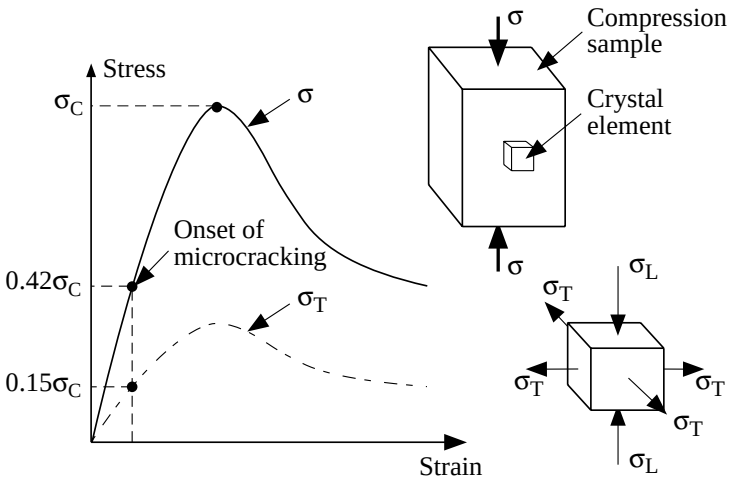

Figure 5: Driving force for triggering damage initiation in compression.

In this study, damage initiation and evolution in a high explosive simulant material are observed experimentally. Such damage is the direct consequence of heterogeneity, or the significant mismatch of the elastic constants between crystal and binder. The mixture theory, which explicitly treats the material as a heterogeneous composite, correctly predicts failure in uniaxial compression sample without resorting to any other artificial mechanisms.

ACKNOWLEDGEMENTS

This study was funded by the Department of Energy and the Department of Defense/Office of Munitions under the Joint DoD/DOE Munitions Technology Development Program.

REFERENCES

1. Chu, T.C., Ranson, W.F., Sutton, M.A. and Peters, W.H. (1985), *Exp. Mech.* 25, 232.
2. Nemat-Nasser, S. and Horii, H. (1982), *J. Geophys. Res.* 87, 6805.
3. Ortiz, M. (1985), *Mech. Mater.* 1, 67.